Cascaded self-Raman lasers based on 382 cm^{-1} shift in Nd:$GdVO_4$

Jipeng Lin* **and Helen M. Pask**

MQ Photonics, Department of Physics and Astronomy, Macquarie University, NSW 2109, Australia
jipeng.lin@mq.edu.au

Abstract: We report quasi-continuous-wave, cascaded Nd:$GdVO_4$ self-Raman lasers based on a secondary Raman transition at 382 cm^{-1} for which the Raman gain was estimated to be 0.7cm/GW. Laser output was obtained in the near-infrared at 1108 nm, 1156 nm and 1227 nm. By incorporating intracavity sum-frequency generation (SFG) or second-harmonic generation (SHG), high power output at four discrete visible wavelengths could be selected, specifically 3.4 W at 542 nm, 2.8 W at 554 nm, 1.4 W at 566 nm and 0.8 W at 577 nm, with corresponding diode-to-visible optical conversion efficiencies of 11.7%, 9.7%, 4.8% and 2.7% respectively.

OCIS codes: (140.3550) Lasers, Raman; (140.3515) Lasers, frequency doubled.

References and links

1. J. A. Piper and H. M. Pask, "Crystalline Raman lasers," IEEE J. Sel. Top. Quantum Electron. **13**(3), 692–704 (2007).
2. A. J. Lee, D. J. Spence, J. A. Piper, and H. M. Pask, "A wavelength-versatile, continuous-wave, self-Raman solid-state laser operating in the visible," Opt. Express **18**(19), 20013–20018 (2010).
3. X. Li, H. M. Pask, A. J. Lee, Y. Huo, J. A. Piper, and D. J. Spence, "Miniature wavelength-selectable Raman laser: new insights for optimizing performance," Opt. Express **19**(25), 25623–25631 (2011).
4. E. Rittweger, K. Y. Han, S. E. Irvine, C. Eggeling, and S. W. Hell, "STED microscopy reveals crystal colour centres with nanometric resolution," Nat. Photonics **3**(3), 144–147 (2009).
5. A. A. Kaminskii, K. I. Ueda, H. J. Eichler, Y. Kuwano, H. Kouta, S. N. Bagaev, T. H. Chyba, J. C. Barnes, G. M. A. Gad, T. Murai, and J. Lu, "Tetragonal vanadates YVO_4 and $GdVO_4$ – new efficient $\chi^{(3)}$ materials for Raman lasers," Opt. Commun. **194**(1-3), 201–206 (2001).
6. T. T. Basiev, A. A. Sobol, P. G. Zverev, L. I. Ivleva, V. V. Osiko, and R. C. Powell, "Raman spectroscopy of crystals for stimulated Raman scattering," Opt. Mater. **11**(4), 307–314 (1999).
7. J. T. Murray, R. C. Powell, and N. Peyghambarian, "Properties of stimulated Raman scattering in crystals," J. Lumin. **66–67**, 89–93 (1995).
8. W. Sun, Q. Wang, Z. Liu, X. Zhang, G. Wang, F. Bai, W. Lan, X. Wan, and H. Zhang, "An efficient 1103 nm Nd: YAG/$BaWO_4$ Raman laser," Laser Phys. Lett. **8**(7), 512–515 (2011).
9. T. T. Basiev, A. A. Sobol, Y. K. Voronko, and P. G. Zverev, "Spontaneous Raman spectroscopy of tungstate and molybdate crystals for Raman lasers," Opt. Mater. **15**(3), 205–216 (2000).
10. Y. F. Chen, K. W. Su, H. J. Zhang, J. Y. Wang, and M. H. Jiang, "Efficient diode-pumped actively Q-switched Nd:YAG/$BaWO_4$ intracavity Raman laser," Opt. Lett. **30**(24), 3335–3337 (2005).
11. J. Lin and H. Pask, "Nd:$GdVO_4$ self-Raman laser using double-end polarised pumping at 880 nm for high power infrared and visible output," Appl. Phys. B (to be published).
12. G. Lu, C. Li, W. Wang, Z. Wang, H. Xia, and P. Zhao, "Raman investigation of lattice vibration modes and thermal conductivity of Nd-doped zircon-type laser crystals," Mater. Sci. Eng. **98**(2), 156–160 (2003).
13. P. G. Zverev, A. Y. Karasik, A. A. Sobol, D. S. Chunaev, T. T. Basiev, A. I. Zagumennyi, Y. D. Zavartsev, S. A. Kutovoi, V. V. Osiko, and I. A. Shcherbakov, "Stimulated Raman scattering of picosecond pulses in $GdVO_4$ and YVO_4 crystals," in ***Advanced Solid-State Photonics***, OSA Technical Digest (Optical Society of America, 2004), paper TuB10.

1. Introduction

Stimulated Raman scattering (SRS) offers a practical and efficient way to generate laser output at "hard to reach" wavelengths in the infrared, visible and UV wavelength regions [1]. In the case of intracavity continuous-wave (CW) Raman lasers where a high-Q cavity is required for the fundamental field to reach the threshold for SRS, high circulating powers at both fundamental and first Stokes wavelengths can enable wavelength-selectable operation at several visible lines through intracavity sum-frequency mixing (SFM); here the SFM crystal

#167864 - $15.00 USD Received 2 May 2012; revised 5 Jun 2012; accepted 6 Jun 2012; published 21 Jun 2012

can be temperature or angle-tuned to phase-match different interactions. This has been demonstrated in the multi-Watt output power regime [2] as well as in a miniature system pumped with only a few Watts of diode power [3]. The "sets" of wavelength-selectable wavelengths that can be generated depend on the Raman shift, and whether it can be cascaded efficiently to higher order Stokes lines. For example the 1332 cm^{-1} shift in diamond can be used to generate 532 nm, 573 nm and 620 nm, while the 882 cm^{-1} shift in Nd:$GdVO_4$ delivers 532 nm, 559 nm and 586 nm. It would however be of considerable interest for example in fluorescence microscopy [4] if a more-closely spaced set of wavelength output across the yellow wavelength band could be generated.

In [5–7], simple covalent crystals such as diamond, or more complex crystals with molecular ionic groupings such as the tungstates, vanadates, molybdates, iodates were recognized as promising candidates for efficient SRS. Typically these materials have Raman spectra where there are only a few, strong, isolated peaks, and it is these peaks that are usually utilized in the development of Raman lasers. However in such crystals, there are frequently weaker Raman transitions, and the usefulness of these has not been widely considered to our knowledge. In [8], a pulsed $BaWO_4$ intracavity Raman laser was reported, operating on the 332 cm^{-1} shift, which from the spontaneous Raman spectra reported in [9] has a Raman gain ~2.5 times smaller than the more widely used, stronger peak at 925 cm^{-1}. That laser, operating at 1103 nm, generated 1.23 W at 17 kHz, which was comparable to other $BaWO_4$ lasers operating at 1180 nm [10]. Recently in our own work [11] on the power scaling of a Nd:$GdVO_4$ self-Raman laser, we observed competition effects between SRS based on the strongest (882 cm^{-1}) shift in Nd:$GdVO_4$ and a weaker transition at 382 cm^{-1}. Specifically, the laser output at 1173nm was found to scale with diode pump power reaching a maximum output power of 4.1 W for a diode pump power of 54 W. At this point a new first-Stokes line at 1108 nm, corresponding to the weaker transition at 382 cm^{-1} was found to reach threshold, causing the output at 1173 nm to roll over. In this paper, we set out to harness this "annoying" Raman transition, and to explore whether it would be possible to use it to build an efficient Raman laser. In part, we were also motivated by the possibilities for combining this relatively small Raman shift with SFM to generate wavelength-selectable laser output at several closely-spaced wavelengths across the yellow spectrum.

In this paper we consider the Raman spectra of Nd:$GdVO_4$, and then report three cases in which separate laser arrangements which have effectively utilized the 382 cm^{-1} shift. All the lasers produce quasi-CW (QCW) laser output, with a duty cycle of 50%, and the powers reported are the instantaneous peak powers (ie the powers during the "on" time). For ***Case 1,*** we report a Raman laser that generates 1.4 W at 1108 nm and 120 mW at 1156 nm, these being the first and second Stokes wavelengths corresponding to the 382 cm^{-1} transition. For ***Case 2***, we report an infrared laser generating 1 W at 1227 nm, this corresponding to two sequential shifts at 882 cm^{-1} (to 1173 nm) followed by 382 cm^{-1} (to 1227 nm). For ***Case 3***, we report a wavelength-selectable Raman laser that incorporates SFM in a BBO crystal, generating laser output at four closely-spaced wavelengths in the lime-yellow region: 3.4 W at 542 nm, 2.8 W at 554 nm, 1.4 W at 566 nm and 0.8 W at 577 nm.

2. Spontaneous Raman spectra for Nd:$GdVO_4$

Polarized spontaneous Raman spectra for Nd:$GdVO_4$ was measured by using a RENISHAW INVIA Raman Spectrometer with 514 nm Argon laser excitation. This spectrometer operates in backscattering mode, and the resolution is <2 cm^{-1}. The measured spectra are shown in Fig. 1, for two configurations. In Fig. 1(a) the excitation beam propagates along the a-axis and is polarized along the c-axes of the Nd:$GdVO_4$ crystal. The Raman signal is the backscattered component with polarization also along the c-axis. In Fig. 1(b) the excitation beam propagates along the c-axis and is polarized along the a-axis of the Nd:$GdVO_4$ crystal. The Raman signal is the backscattered component with polarization also along the a-axis. The corresponding Porto notations for the two configurations are $X(ZZ)\overline{Y}$ and $X(YY)\overline{Z}$, and

#167864 - $15.00 USD Received 2 May 2012; revised 5 Jun 2012; accepted 6 Jun 2012; published 21 Jun 2012

these configurations were chosen because they correspond to orientations that are best suited for oscillation. Comparing Fig. 1(a) and Fig. 1(b), we see that the c-polarized spectra exhibits simpler spectra featuring two main peaks at 882 cm^{-1} and 382 cm^{-1}, each of which is stronger than for the case of a-polarized spectra. Since the steady-state Raman gain is directly proportional to the peaks of the Raman spectra [6], and the steady-state Raman gain g_R for 882 cm^{-1} was reported to be 4.5 cm/GW [5], we can therefore estimate g_R to be ~0.7 cm/GW for 382 cm^{-1} for the X(ZZ) $\overline{X}$ configuration. Fortunately this configuration is the one used in the vast majority of self-Raman lasers.

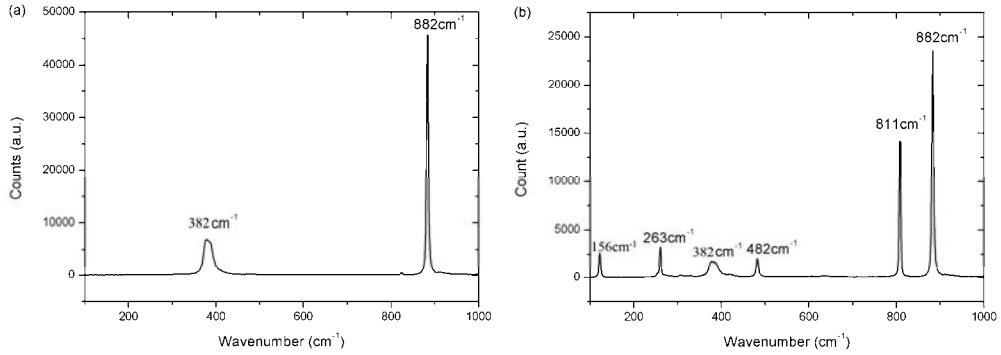

Fig. 1 Nd:$GdVO_4$ polarized Raman spectrum (a) along c-axis with scattering configuration X(ZZ) $\overline{Y}$, and (b) a-axis of with scattering configuration X(YY) $\overline{Z}$.

Our observations of Raman spectra for Nd:$GdVO_4$ are broadly consistent with those made elsewhere for $GdVO_4$ and Nd:$GdVO_4$ [5, 12, 13] although we were unable to find measurements of our exact configurations to compare. In particular, in [12], the primary Raman peak at ~882cm^{-1} was assigned to a V-O stretching mode, while the secondary peak at ~382 cm^{-1} was assigned to an O-V-O bending mode.

3. Experiment

A schematic diagram for the self-Raman laser systems studied here is shown in Fig. 2. A 20 mm long 0.3% Nd:$GdVO_4$ crystal was used as the self-Raman medium. One end was coated (M1) for high-transmission for the pump diode (HT>90% at 880nm), and high-reflectivity for the fundamental and Stokes wavelengths encountered here (HR>99.99% at 1063-1227nm).

A 60 W 880 nm high-brightness LD (Φ = 100 μm, 0.22 N.A.) was used as the pumping source. After being collimated with a 25 mm lens, the pumping beam was then separated by a beam splitting cube into two beams having nearly equal power but orthogonal polarizations. A half-wave plate was used to rotate the polarization of one beam by 90° so that the polarization directions of both beams were parallel to the c-axis of Nd:$GdVO_4$ crystal. The collimated pumping beams were then focused with 100 mm converging lenses into each end of the Nd:$GdVO_4$ crystal, delivering pump spot sizes (radii) of ~200 μm. Approximately 99% of the incident pump power was absorbed within the crystal using this pumping scheme. This 880 nm double-end polarized pumping scheme been evaluated in detail elsewhere [11] and found to have several advantages over conventional single-end unpolarized pumping, namely 25% higher absorption of pump power, lower on-axis temperature in the Nd:$GdVO_4$ crystal and 60% higher mode matching between the pump and fundamental beams. The resonator was found to be very sensitive to the strong thermal lens in the Nd:$GdVO_4$ self-Raman crystal, and for this reason the laser was operated at 50% duty cycle. QCW operation was realized by placing a chopper (1 kHz, 50% duty-cycle) just in front of the fiber output.

A V-shaped laser resonator was formed by the direct coating (M1) on the Nd:$GdVO_4$ crystal, a flat folding mirror (M2) and an output coupler (OC). For ***Case 1*** to investigate laser performance at the 1108 nm first and 1156 second-Stokes wavelengths, we chose a plane fold

#167864 - $15.00 USD Received 2 May 2012; revised 5 Jun 2012; accepted 6 Jun 2012; published 21 Jun 2012

mirror M2 for which we could optimize the fold angle and introduce sufficient transmission loss at 1173 nm to suppress the stronger 882 cm^{-1} shift. Accordingly, the fold angle was 40°, and M2 had high reflectivity (HR>99.99%) from 1063 nm to 1156 nm, 2.2% transmission at 1173 nm, high-transmission HT>90% at 880 nm, and HT>80% from 532 to 570 nm. We used an OC (ROC = 300 mm) having T~0.1% at 1063 nm, 1108 nm and 1156 nm. For ***Case 2***, of the laser operating at 1227 nm, the fundamental 1063 nm was first shifted to 1173 nm by utilizing 882 cm^{-1} shift and subsequently cascaded to 1227 nm by utilizing 382 cm^{-1} shift. Here we used a different plane fold mirror M2 and optimized the fold angle to suppress 1308 nm, the second-Stokes wavelength corresponding to the 882 cm^{-1}. Accordingly the fold angle was 38° and M2 had high reflectivity (HR>99.99%) from 1063 nm to 1227 nm, HT>90% at 880 nm, HT>80% from 532 to 570 nm and T>20% at 1308. A different OC having 300 mm concave radius of curvature, high reflectivity (R>99.99%) at 1063 nm and 1173 nm, and transmission of 0.1% at 1227 nm was used. For ***Case 3***, in which visible operation was investigated, we used the same plane M2 and 300 mm OC used in ***Case 1.*** The intracavity SFM was realized by using a 3 mm BBO crystal cut for type-I phase-matching ($\theta = 22.1°$, $\varphi = 0°$), placed between M2 and the OC. BBO was chosen in this case because of its short length. The visible emission was coupled from both sides of BBO crystal through M2 and the OC, and the output powers reported for each visible wavelength is the sum of the powers measured through M2 and OC. In future, it should be possible to achieve single-ended output by sourcing mirrors with appropriate transmission. The length of the cavity arm M1M2 was fixed at 30 mm for three cases. The cavity length was ~50 mm for infrared operation and was lengthened slightly to ~60 mm in order to accommodate the BBO crystal. Accordingly the TEM_{00} mode radius in the laser media was ~180 μm for infrared operation and ~190 μm for visible operation.

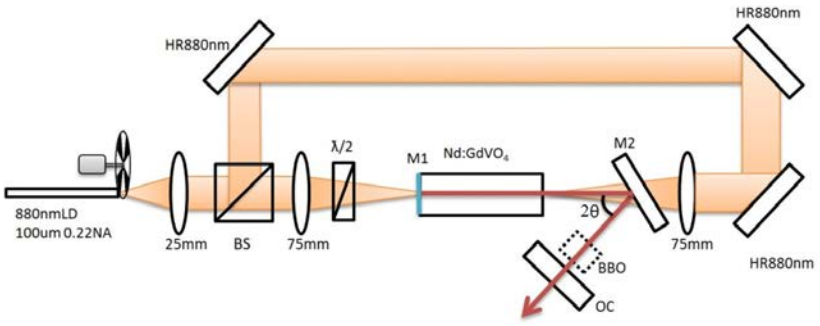

Fig. 2. Schematic diagram of cascaded Nd:$GdVO_4$ self-Raman laser utilizing 382 cm^{-1} shift.

4. Results

4.1 Case 1: Laser operating at 1108 and 1156 nm utilizing the 382cm $^{-1}$ shift

The performance of the laser operating at first (1108 nm) and second-Stokes (1156 nm) wavelengths is shown in Fig. 3(a). Threshold for SRS was reached for an absorbed diode pump power of 5.5 W and the first Stokes output at 1108 nm reached a maximum of 1.41 W, for 30 W absorbed pump power. For this pump power, the corresponding intracavity circulating power at 1108 nm was 1400 W, and this was sufficient for the second-Stokes line at 1156nm to reach threshold. As can be seen in Fig. 3(a), the intracavity power of 1108 nm did not rise significantly above this level. The highest output power obtained at 1156 nm was 120 mW, for an absorbed pump power of 34 W. Beyond this pump power, the powers of first and second Stokes began to decrease, which we attribute to strong thermal lensing in the self-Raman crystal making the resonator become unstable.

The optical spectrum for the IR outputs were measured with a high-resolution optical spectrometer (Ocean-optics HR4000, 0.09nm resolution), and the fundamental, first and

#167864 - $15.00 USD Received 2 May 2012; revised 5 Jun 2012; accepted 6 Jun 2012; published 21 Jun 2012

second Stokes each had linewidth of around 0.5 nm. The beam quality M^2 factors were 5.4 for 1108 nm and 3.5 for 1156 nm by using a beamscope (Gentec-Beamscope-P7). These measurements were made at maximum output power.

4.2 Case 2: Laser operating at 1227 nm utilizing the 882 cm $^{-1}$ and 382 cm $^{-1}$ shifts

When the laser was re-configured to obtain output at 1227 nm using sequential Raman shifts of 882 cm^{-1} (to 1173 nm) and 382 cm^{-1} (to 1227 nm), the thresholds for the fundamental 1063nm, first-Stokes 1173 nm and second-Stokes 1227 nm, were found to correspond to absorbed pump powers of 0.2 W, 0.9 W and 3.1 W respectively. The laser performance is shown in Fig. 3(b). For QCW operation, the maximum output peak power at 1227 nm was 1.01 W with 37 W absorbed pump power.

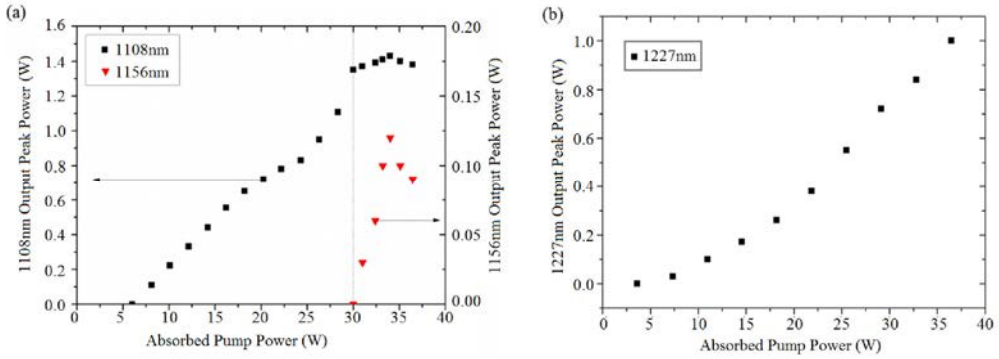

Fig. 3. Laser output power of (a) 1108 nm and 1156 nm utilizing the 382 cm^{-1} shift, and (b) 1207 nm utilizing 882 cm^{-1} and 382 cm^{-1} shifts.

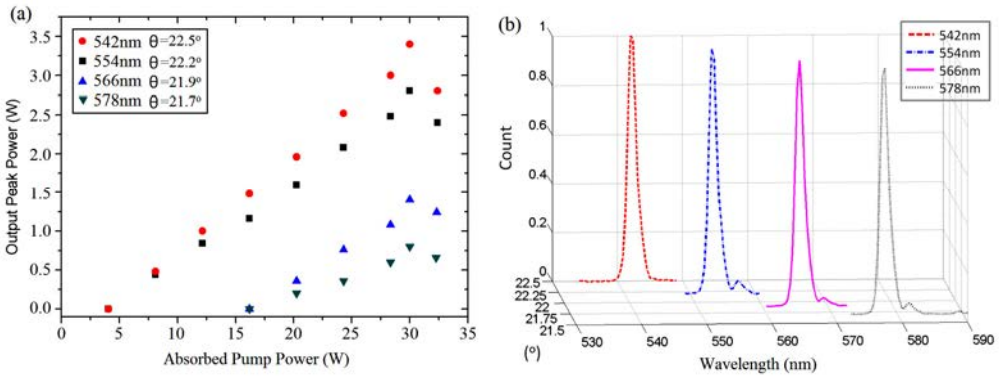

Fig. 4. (a) Laser output powers at the 4 visible wavelengths, obtained by angle tuning the BBO crystal and (b) corresponding optical spectra.

4.3 Case 3: Wavelength-selectable output in the visible utilizing the 382 cm $^{-1}$ shift

The laser performance for visible generation is shown in Fig. 4(a). Because the output coupler used for visible generation had much higher reflectivity (HR>99.99% @1063-1156nm) than that used for coupling first-Stokes (T = 0.1% @1063, 1108 and 1156 nm), the first- and second-Stokes had much lower SRS threshold, i.e. 4.05 W for 1108 nm and 16.2 W for 1156 nm. The corresponding intracavity powers required for reaching SRS threshold were ~800 W at 1063 nm for first-Stokes and ~1100 W at 1108 nm for second-Stokes respectively. By tuning the angle of BBO, four different visible lines could be obtained through intracavity SFM. The combinations of infrared fields that were summed, and the laser performance for

#167864 - $15.00 USD Received 2 May 2012; revised 5 Jun 2012; accepted 6 Jun 2012; published 21 Jun 2012

each of these is summarized in Table 1 in terms of output power, slope efficiency, conversion efficiency, linewidth and beam quality. The maximum output powers were 3.4 W at 542 nm, 2.8 W at 554 nm, 1.4 W at 566 nm and 0.8 W at 577 nm, with corresponding diode-to-visible optical conversion efficiencies of 11.7%, 9.7%, 4.8% and 2.7% respectively. The beam quality factor M^2 was close to 1 near SRS threshold and varied from 3.8 to 5.5 at the highest output powers. The optical spectra of visible output were measured with an optical spectrometer (Ocean-Optics USB2000), as is shown in Fig. 4(b). Note that the linewidths are instrument limited; the resolution of this spectrometer was ~2 nm. The maximum powers of visible lines were achieved at about 30 W pump power, and above this the output power started to roll over due to the strong thermal lensing. Note the roll over point for the visible output powers occurred for lower pump powers than was the case for infrared operation, which is due to the relatively longer cavity length required to accommodate the nonlinear crystal.

Table 1. Summary of laser output performance at four visible lines.

Visible Wavelength	*542 nm*	*554 nm*	*566 nm*	*578 nm*
IR lines for SFM (nm)	1063 + 1108	1108 + 1108	1108 + 1156	1156 + 1156
Maximum Output Power (W)	3.4	2.8	1.4	0.8
Slope Efficiency	11.5%	9.5%	9.7%	5.5%
LD-Visible Efficiency	11.7%	9.7%	4.8%	2.7%
SRS Threshold (W)	4.05	4.05	16.2	16.2
Linewidth (nm)	2.1	2.2	2.4	2.1
M^2 at Highest Output Power	5.5	5.1	4.3	3.8

7. Conclusion

We have, for the first time to our knowledge, utilized the 382 cm^{-1} Raman transition in Nd:$GdVO_4$ in a Raman laser. The Raman gain for this transition was estimated to be 0.9 cm/GW based on comparison of the peaks in the spontaneous Raman spectrum, and the Raman gain coefficient for the stronger 882 cm^{-1} which was determined to be 4.5 cm/GW in [5]. First and second Stokes output at 1108 nm and 1156 nm respectively were observed corresponding to the 382 cm^{-1} shift, with a maximum QCW output power of 1.4 W. Laser performance was also achieved in the infrared at 1227 nm using sequential Raman shifts at 882 cm^{-1} and 382 cm^{-1}; 1 W of QCW output was obtained at this wavelength. In the visible, we have demonstrated QCW operation on four visible lines outputs from a cascaded 382 cm^{-1} Nd:$GdVO_4$ self-Raman laser incorporating intracavity SFG/SHG. Four discrete visible lines were generated, with the maximum output powers of 3.4 W at 542 nm, 2.8 W at 554 nm, 1.4W at 566 nm and 0.8 W at 577 nm, and corresponding diode-to-visible optical conversion efficiencies of 11.7%, 9.7%, 4.8% and 2.7% respectively. Compared to most crystalline Raman lasers in which the Raman shift is around 750 cm^{-1} to 900 cm^{-1}, this system using the shorter 382 cm^{-1} shift can generate more visible lines in green-lime-yellow regions, which could be of interest for biophotonics applications where new wavelengths are required to match a growing range of chromophores. There are several prospects for improving the performance of this laser, in particular to realize CW operation and achieve lower thresholds, both through optimizing the coatings on the resonator mirrors, and by improvements to the resonator design. Given the relatively low Raman gain for the 382 cm^{-1} shift, it would be desirable to engineer smaller spot size in the Raman crystal, however this would further exacerbate the thermal loading that limits CW operation of the self-Raman laser. Therefore we suggest it may be desirable to use separate Raman and laser crystals and design a resonator with large spot size in the laser crystal (which could be Nd:$GdVO_4$ or some other crystal such as Nd:YLF) and an undoped $GdVO_4$ crystal as the Raman crystal.

#167864 - $15.00 USD Received 2 May 2012; revised 5 Jun 2012; accepted 6 Jun 2012; published 21 Jun 2012

Optics Express

Title Details

Related Titles

- **Alternative Media Edition** (1)
- **Supplement** (1)

Lists

Marked Titles (0)

Search History

1094-4087
0048-9697
1068-7971
0898-929X
1039-7116
1471-2164
0094-8276
1279-7707

Basic Description

Title	Optics Express
ISSN	1094-4087
Publisher	Optical Society of America
Country	United States
Status	Active
Start Year	1997
Frequency	Bi-weekly
Language of Text	Text in: English
Refereed	Yes
Abstracted / Indexed	Yes
Open Access	Yes http://www.opticsexpress.org
Serial Type	Journal
Content Type	Academic / Scholarly
Format	Online
Website	http://www.opticsinfobase.org/oe/journal/oe/about.cfm
Email	opex@osa.org
Description	Covers original research in optical science and technology.

- **Subject Classifications**
- **Additional Title Details**
- **Publisher & Ordering Details**
- **Online Availability**
- **Abstracting & Indexing**
- **Other Availability**
- **Demographics**
- **Reviews**

Save to List Email Download Print Corrections Expand All Collapse All